

Intercomparison of reflectances observed by GOME and SCIAMACHY in the visible wavelength range

Lieuwe G. Tilstra and Piet Stammes

We compare the Earth reflectances of the spectrometers Global Ozone Monitoring Experiment (GOME) and Scanning Imaging Absorption Spectrometer for Atmospheric Chartography (SCIAMACHY) over their overlapping wavelength range (240–800 nm). The goal is to investigate the quality of the radiometric calibration of SCIAMACHY using calibrated GOME data as a reference. However, severe degradation of the GOME instrument in the UV since 2001 prevents it from being a reliable reference below 500 nm. Above 500 nm, GOME is reliable and we find substantial disagreement between GOME and SCIAMACHY, of the order of 15%–20%, which we can attribute completely to the current calibration problems of SCIAMACHY. These numbers are supported by a previous study in which SCIAMACHY was compared with the imager Medium Resolution Imaging Spectrometer (MERIS) onboard the Envisat satellite. © 2006 Optical Society of America
OCIS codes: 280.0280, 010.0010.

1. Introduction

Absolute calibration of the reflectance is important for a number of atmospheric products that are retrieved from measurements by the satellite UV–visible spectrometers Global Ozone Monitoring Experiment (GOME),¹ Scanning Imaging Absorption Spectrometer for Atmospheric Chartography (SCIAMACHY),² and Ozone Monitoring Instrument.³ Although retrievals of column densities of trace gases, such as ozone and NO₂ using the differential optical absorption spectroscopy method,⁴ are insensitive to errors in the absolute calibration of the reflectance, other products, such as the retrieval of the vertical distribution of ozone,^{5–10} the retrieval of cloud properties,^{11,12} and aerosol retrieval¹³ are highly sensitive. For these retrievals a thorough preflight instrument calibration and an in-flight instrument monitoring to follow the degradation of the optics are both essential.

In-flight calibration, whether it is to monitor the effects of degradation or to correct preflight calibration errors, or shifts in these calibrations after launch, can

be performed in a number of ways. First, a common approach for reflectance validation is that of satellite intercomparison. This of course requires one of the instruments to have a known calibration accuracy. Second, radiative transfer models can be used in combination with certain target sites (usually cloud-free desert sites) when the site's simulated reflectance is compared with that measured by the satellite instrument in question.¹⁴ These comparisons may even be automatized to cover a larger set of observations over a larger period of time.¹⁵

This paper is devoted to a satellite intercomparison between two spectrometers, namely, GOME¹ onboard the ERS-2 satellite and SCIAMACHY² onboard the Envisat satellite. The higher spatial resolution of SCIAMACHY allows a reflectance comparison with high accuracy, provided that we restrict ourselves to scenes without clouds with a homogeneous surface. Studies like this, involving a comparison between GOME and SCIAMACHY, have been attempted before,¹⁶ but they were not as extensive as the present work.

The outline of the paper is as follows. Section 2 introduces the two spectrometers, GOME and SCIAMACHY. In Section 3 we introduce the applied method of comparing the two spectrometers and present the results. Sections 4 and 5 deal with two complications that affect the accuracy of this specific comparison: degradation of the optics of the GOME instrument and the time delay between the overpasses of the two satellites that alters the scattering

The authors are with the Royal Netherlands Meteorological Institute, P.O. Box 201, NL-3730 AE De Bilt, The Netherlands. L. G. Tilstra's e-mail address is tilstra@knmi.nl.

Received 11 August 2005; revised 18 November 2005; accepted 22 December 2005; posted 11 January 2006 (Doc. ID 64073).

0003-6935/06/174129-07\$15.00/0

© 2006 Optical Society of America

geometry. Finally, a short summary of the results is given in Section 6.

2. Description of GOME and SCIAMACHY

A. GOME

GOME¹ was launched in April 1995 as a small-scale version of the spectrometer SCIAMACHY.² GOME, onboard ERS-2, measures the Earth's radiance and the solar irradiance in the UV-visible spectral range of 240–795 nm at a spectral resolution of 0.2–0.4 nm. The ERS-2 satellite is in a near-polar, Sun-synchronous orbit with an orbital period of around 100 min. The local crossing time of the descending node at the equator is 10:30 a.m.

During its flight, GOME is observing the Earth in the along-track direction by the movement of the satellite and in the across-track direction by the movement of its scan mirror. This mirror scans back and forth in a time period of 6.0 s, of which 4.5 s are spent scanning in the forward direction, when the instrument is scanning the Earth's surface from east to west. After this forward scan, a fast reverse scan takes the mirror back to its starting position. Depending on the scan direction, the swath is either comprised of three forward pixels, called east, nadir, and west (forward scan) or of one large backscan pixel (backward scan). The forward pixels cover approximately 320 km × 40 km of area; the backscan pixels cover roughly 960 km × 40 km. Global coverage of the Earth is achieved in a 3 day period.

The main level 2 products of GOME are the global distributions of total column amounts of ozone and NO₂. Other products that have been successfully extracted from the data are the trace gases OCIO, SO₂, H₂CO, and BrO; cloud properties; aerosol presence; and ozone vertical profiles.

B. SCIAMACHY

SCIAMACHY² was launched on 1 March 2002 onboard the Envisat satellite. Like GOME, it was launched into a near-polar, Sun-synchronous orbit, with an identical orbital period of ~100 min. The local crossing time of the equator is 10:00 a.m., so SCIAMACHY observes a certain ground scene 30 min in advance of GOME. A major difference with respect to GOME is that SCIAMACHY has the ability to perform not only nadir measurements but also limb measurements. These two measurement modes are being alternated along the orbit. The resulting data are stored in blocks, called states. A nadir state covers an area of 960 km × 490 km (across track multiplied by along track).

The wavelength region covered by SCIAMACHY is 240–2380 nm, with a spectral resolution of 0.2–1.5 nm. The scanning sequence is similar to that of GOME: 4 s forward scan and a fast reverse scan in 1 s. The swath is 960 km wide, equal to that of GOME. A major difference with GOME is that the nadir spectrum is divided into 56 wavelength regions, called clusters, that are all read out with their own integration time (IT). This allows a higher spatial

resolution for the most important spectral regions, at the expense of other wavelength regions where the spectrum is of less scientific interest or would otherwise yield a weak signal. Typical ITs are 0.25 s (pixel size, 60 km × 30 km) and 1.0 s (pixel size, 240 km × 30 km), but 0.125, 0.5, 5, and 10 s are also used. Because of the alternation of nadir and limb modes, global coverage is achieved in only 6 days instead of 3 days for the GOME instrument.

As for the level 2 products of SCIAMACHY, the extension of the Earth's radiance spectrum to wavelengths above 800 nm enables the detection of trace gases absorbing in the near IR, including CO, CO₂, CH₄, and N₂O. The limb measuring mode enables measurements of the vertical distribution of all retrieved trace gases.

3. Intercomparison

A. Method

The method we use relies on the fact that the spatial resolution of the SCIAMACHY instrument is generally higher than that of GOME (see Section 2). This makes it possible to create almost identical areas covered by GOME and SCIAMACHY pixels and to directly compare the associated top-of-the-atmosphere (TOA) reflectances with each other. In this paper the reflectance is defined as

$$R = \frac{\pi I}{\mu_0 E}, \quad (1)$$

where I is the TOA radiance reflected by the Earth's atmosphere (in $\text{Wm}^{-2} \text{nm}^{-1} \text{sr}^{-1}$), E is the incident extra-atmospheric solar irradiance at the TOA perpendicular to the solar beam (in $\text{Wm}^{-2} \text{nm}^{-1}$), and μ_0 is the cosine of the solar zenith angle θ_0 .

The procedure for comparing the reflectances is explained more clearly in Fig. 1. Here we have plotted the coverage of two SCIAMACHY states, taken from orbit 2509 dated 23 August 2002. For the upper state we plotted the pixels of the wavelength clusters measured with a 1.0 s IT; in the lower state the pixels are those of the 0.25 s IT clusters. Not shown are the individual GOME pixels, which are from orbit 38,381. However, the black box in the lower state indicates the area that is being covered by nine subsequent GOME nadir pixels. Its size is approximately 320 km × 410 km. For this area, we can calculate a mean GOME reflectance.

To arrive at a similar SCIAMACHY reflectance of the same region, the area is tessellated with the available SCIAMACHY pixels. The overlap fraction of the SCIAMACHY pixels with the GOME area is recorded and serves as a weighting factor for the calculation of the mean SCIAMACHY reflectance. Within the uncertainty of this method of comparison, the GOME and SCIAMACHY reflectances should be identical if both instruments are calibrated correctly. Figure 2 shows the result of a reflectance comparison of a nadir area over part of the Sahara Desert.

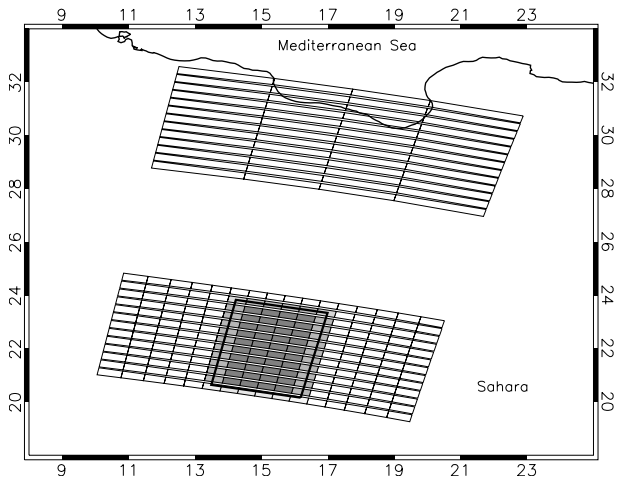


Fig. 1. Method used to compare the reflectances measured by GOME and SCIAMACHY. The picture shows two blocks of SCIAMACHY data (these blocks are called states). In the upper state we plotted SCIAMACHY pixels of 1.0 s IT. In the lower state we selected SCIAMACHY pixels of 0.25 s IT and we combined nine subsequent nadir GOME ground pixels into an area of $\sim 320 \text{ km} \times 410 \text{ km}$ (delineated by thick black lines), yielding an accumulated mean GOME reflectance. This region is then tessellated with SCIAMACHY ground pixels in such a way that the relative contribution of a ground pixel to the accumulated SCIAMACHY reflectance is proportional to its overlap with the GOME area. After this, the two reflectances may be compared.

B. Accuracy

There are a number of aspects that determine the accuracy of this type of comparison. First, the tessellation procedure itself is a source of errors because the SCIAMACHY pixels do not perfectly match the GOME area (see Fig. 1). This is corrected for homogeneous scenes by counting only the fraction of the SCIAMACHY pixels that are inside the GOME region. However, this does not account for a possible inhomogeneity over the area covered by the SCIAMACHY pixels. We estimate the error in the reflectance due to this mismatch to be less than a

few percent. However, this error is reduced considerably over homogeneous scenes.

The second source of error is caused by scene changes in the time period of 30 min between the overpasses of GOME and SCIAMACHY. These scene changes are mostly caused by the movement of clouds. In the pessimistic case of a thick cloud (spectral albedo of ~ 0.8) entering a cloud-free ocean scene (TOA albedo of ~ 0.1) with a speed of $\sim 60 \text{ km/h}$ and covering 3 of the 55 SCIAMACHY pixels (see Fig. 1), this would result in an error of roughly $3/55 \times (0.8 - 0.1) \approx 4\%$ in the GOME–SCIAMACHY comparison. For this reason, clouded scenes were avoided in the comparison.

Third, because of the same time delay, the solar angles with respect to the ground scene are different for GOME and SCIAMACHY. We will study the consequences of this effect in Section 5. For the moment it is sufficient to know that the effects will turn out to be small.

C. Results

Figure 3 shows the main result of the reflectance comparison presented in this paper. On the vertical axis we plotted the ratio of the reflectances of GOME and SCIAMACHY for the three viewing directions (or pixel types) of GOME (east, nadir, west). We used SCIAMACHY orbit 2509, dated 23 August 2002, and GOME orbit 38,381, of the same day, following the track of the SCIAMACHY orbit. The GOME data were generated by processor version 2.10; the SCIAMACHY data were produced by software version 5.00. We focused on a region over the Sahara Desert, shown in Fig. 1, which was unclouded at the time of measurement. Furthermore, the surface albedo is more or less constant over the area, which improves the accuracy of the comparison.

The result of Fig. 3 shows that there is disagreement between GOME and SCIAMACHY over the entire wavelength range. Above $\sim 500 \text{ nm}$, the ratios of different viewing directions are equal, at least within

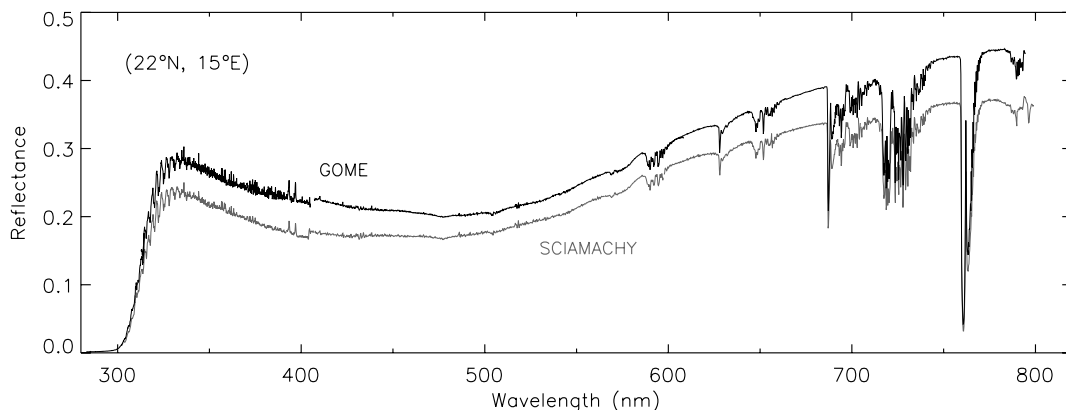


Fig. 2. Reflectances measured by SCIAMACHY and GOME as a function of wavelength for the same Earth scene over part of the Sahara Desert (see Fig. 1). The SCIAMACHY reflectance is systematically lower than the GOME reflectance by typically 20%, depending on the wavelength. Note that there are no signs of an etalon effect in the GOME reflectance (compare with Fig. 4), which would have been the case if we had used the official, out-of-date solar irradiance spectrum.

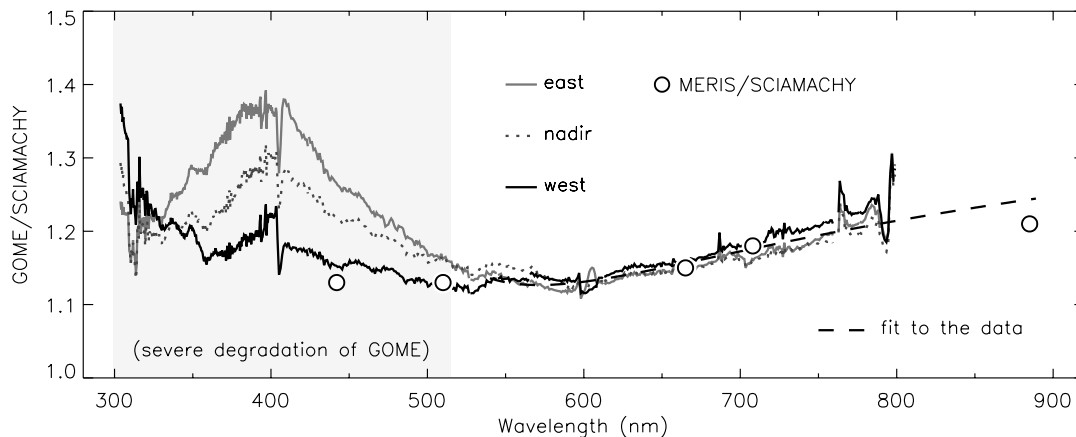


Fig. 3. Ratio of the reflectances of GOME and SCIAMACHY for three homogeneous regions over the Sahara Desert, corresponding to the three viewing directions (or pixel types) of GOME (these are east, nadir, and west). The shaded area left of ~ 500 nm corresponds to the wavelength region that is not to be trusted because of (scan-mirror-dependent) degradation of the GOME reflectance. Above ~ 500 nm the GOME/SCIAMACHY ratios for the three viewing directions are in agreement. The circles indicate the reflectance ratio MERIS/SCIAMACHY on the basis of a comparison between the imager MERIS and SCIAMACHY. These points agree with the GOME and SCIAMACHY points, indicating that SCIAMACHY is the instrument responsible for the discrepancies found in the satellite intercomparison. The dashed curve is a fit to the data above 520 nm.

the accuracy of the method. Below ~ 500 nm, there appears to be a viewing direction dependency. However, this dependency is caused by degradation of the GOME reflectance. This degradation is known to be scan mirror dependent.¹⁷ A correction for this degradation of the reflectance does exist,⁸ but this correction can be applied only up to 390 nm and is available only for data up to the end of 2001. As a result, we must regard the ratio for wavelengths below ~ 500 nm in Fig. 3 as unfit for drawing conclusions about the quality of the SCIAMACHY radiometric calibration.

On the other hand, the GOME data above ~ 500 nm are reliable, as is evidenced by the fact that the different GOME viewing directions lead to almost the same ratio. Further evidence for the correctness of the ratio, and support for interpreting the ratio as a necessary correction factor on the radiometric calibration of SCIAMACHY, is found in a recent study on a comparison between SCIAMACHY and the Medium Resolution Imaging Spectrometer (MERIS) imager.¹⁸ MERIS, like SCIAMACHY, is onboard the Envisat satellite. The ratios of the reflectances of MERIS and SCIAMACHY are plotted in Fig. 3 as circles. Obviously, these points agree well with the GOME–SCIAMACHY curves. Since GOME and MERIS are both assumed to be calibrated correctly,^{19,20} at least above ~ 500 nm in the case of GOME, the agreement between the MERIS points and the results of this study indicates that SCIAMACHY has a substantial calibration problem, at least in the wavelength region of 500–800 nm.

The whole analysis was repeated for a number of other (cloud-free) scenes, including vegetation, ocean, and other desert scenes. The results agree with the result presented in Fig. 3, with small deviations (up to $\pm 2\%$) around 400 nm and higher deviations around 700 nm (up to $\pm 4\%$). These deviations are

most likely the result of inhomogeneity in the scenes or the presence of thin clouds, effects discussed in Section 3, and effects that are indeed becoming more important at longer wavelengths. Despite the limited number of available cloud-free scenes, the results indicate that the GOME/SCIAMACHY ratio does not depend on the reflectance (or radiance). Since we have high trust in the homogeneous desert scene, we present Fig. 3 as the main result of this paper. A fit $y = a_0 + a_1/(\lambda - \lambda_0) + a_2/(\lambda - \lambda_0)^2$ to the result above 520 nm is also presented in Fig. 3, as a dashed curve, with coefficients $a_0 = 1.47$, $a_1 = -150$, $a_2 = 1.66 \times 10^4$, and $\lambda_0 = 350$ nm. Occasional jumps caused by channel overlaps and gaseous absorption bands were removed from the ratio before the actual fitting. Note that other studies^{14,15,21,22} point to similar calibration errors of SCIAMACHY in the UV and visible.

4. Degradation and Solar Irradiance Issues

During its lifetime, GOME has suffered considerable degradation of its optical components.¹⁹ A complete record of this instrument degradation is recorded by the daily measurements of the solar irradiance. The solar irradiance can be corrected using this record under the assumption that the Sun may serve as a stable reference. The same correction factor is applied to the radiance signals. From the definition of the reflectance [see Eq. (1)] it is clear that the applied corrections cancel out and that the reflectance remains unchanged. However, because the light path for the Earth's radiance measurements is not exactly the same as for the solar irradiance measurements, the radiance signals do not degrade in exactly the same manner as the irradiance signals. Hence, in reality the reflectance does degrade, but a complete correction for this phenomenon is not available at this time.

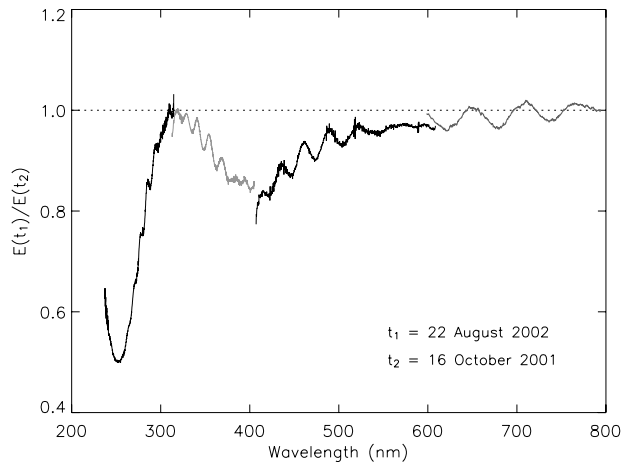


Fig. 4. Degradation of the solar irradiance measurements by GOME. The curve is the ratio between the custom-made solar irradiance spectrum, made up of GOME solar measurements of 22 August 2002, and the official solar irradiance spectrum provided in the GOME L1 data product of the same day, which was in fact measured on 16 October 2001. The oscillating behavior is the result of what is called the etalon effect, which is caused by the gradual buildup of an ice layer on the GOME detectors. The broadband deviation of the ratio from 1 is caused by degradation of the optical components between 16 October 2001 and 22 August 2002. Especially in the UV, this degradation is severe.

Another issue is the fact that, since October 2001, solar irradiances measured by GOME are affected by a pointing problem of the ERS-2 platform. As a result, the official data of the orbit we used contains Earth's radiance data of the day of measurement (in this case 23 August 2002), but a solar irradiance spectrum from 16 October 2001. However, using the raw GOME solar irradiance measurements for 22 August 2002, less than one day before the GOME orbit of the comparison of Section 3, we were able to construct a proper solar irradiance spectrum. This solar irradiance spectrum is the one that is used in the comparison.

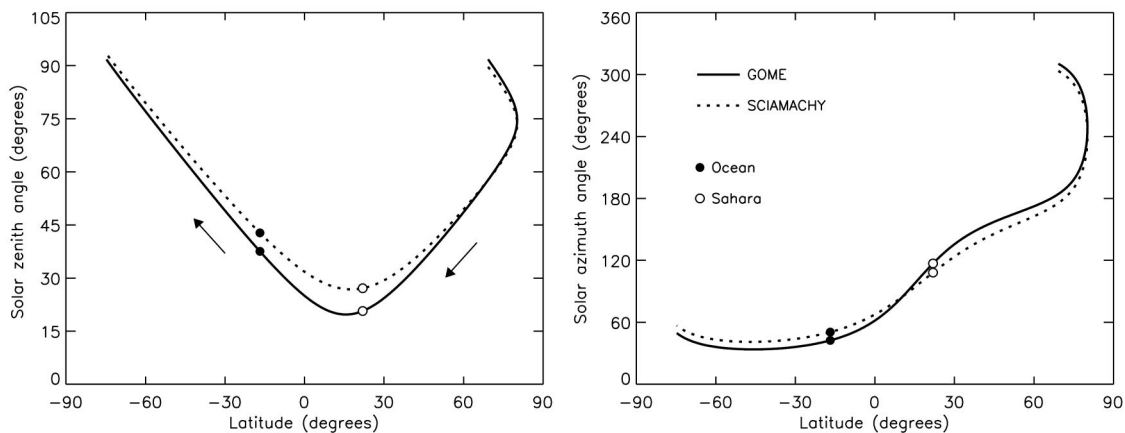


Fig. 5. Solar geometry (θ_0 , ϕ_0) along the orbits of GOME and SCIAMACHY when both instruments observe the same ground scene in exact nadir view (SCIAMACHY does this 30 min in advance of GOME). The circles indicate the solar angles for two specific scenes along the orbit, one over the ocean (16.8°S, 6.4°E) and one over the Sahara region of Fig. 1. Reflectance error estimates caused by differences in observed solar geometry by GOME and SCIAMACHY are given in Fig. 6.

Figure 4 shows the ratio between the solar irradiance spectrum measured on 22 August 2002 and the official solar irradiance spectrum, which is from 16 October 2001. Different types of gray are used to distinguish the four spectral channels of the GOME spectrometer. The first conclusion is that the difference between the two solar spectra is quite large (>10%) below ~500 nm. Second, the ratio contains oscillations. This behavior is caused by what is known as the etalon effect, which is spectral interference by a growing ice layer on top of the detector pixels.

This etalon effect is present in all GOME reflectance spectra after October 2001, unless a recent solar irradiance spectrum is used. Note that with our approach we do remove the etalon effect from the spectra, but we do not remove all types of degradation in the reflectance. Especially in the UV there is a scan-mirror-dependent degradation in the GOME reflectance, shown in Fig. 3 and reported by Van der A *et al.*⁸ For that reason, in Section 3 we focused our comparison on the wavelength region of 500–800 nm, where GOME does not suffer much from the effects of degradation. For SCIAMACHY, degradation is not really an issue because the instrument has proved to be stable and the data we use are from only half of a year after the launch.

5. Effect of a Different Solar Geometry

Because of the 30 min time delay between GOME and SCIAMACHY, the solar angles with respect to the observed ground scene are different. Figure 5 presents the solar zenith angle θ_0 and solar azimuth angle ϕ_0 for both instruments along the same orbit track. The angles were calculated for the nadir pixels from geolocation and overpass time to enable a direct comparison between GOME and SCIAMACHY (which both have different definitions of the solar and viewing angles in their data products).

To estimate the errors that were introduced in the comparison by the difference in solar geometry, we set

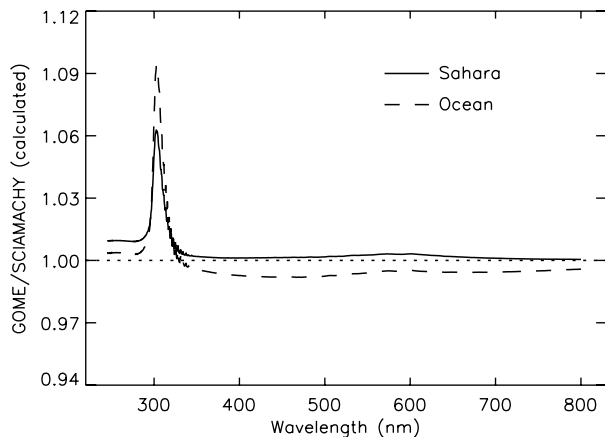


Fig. 6. Calculated effect of the difference in solar geometry on the relative reflectance when GOME and SCIAMACHY observe the same scene (in exact nadir view, compare with Fig. 5).

up a number of simulations, all run by the radiative transfer code Doubling-Adding KNMI (Royal Netherlands Meteorological Institute) (DAK).^{23,24} This radiative transfer model includes polarization, Lambertian surface reflection, ozone absorption, clouds, and aerosols. We selected two scenes from the aforementioned orbits, both unclouded, with one over the ocean (16.8°S, 6.4°E) and the other one being the Sahara scene used in Figs. 1–3. The solar angles of these scenes are indicated in Fig. 5 as the open or solid circles (see legend).

Regarding the DAK input parameters, we assumed Lambertian surface albedos and determined the spectral surface albedos from the GOME Lambert-equivalent reflectivity database.²⁵ The ozone column values are available from either GOME or SCIAMACHY measurements and were in this case obtained from the Troposphere Emission Monitoring Internet Service website.^{8,26–28} For the ozone profiles we assumed a standard mid-latitude summer profile²⁹ for both the ocean and the Sahara sites. After this, the radiative transfer code calculated the reflectances for the two scenes for the geometries of GOME and SCIAMACHY. The ratios between the simulated reflectances are shown in Fig. 6, where the dashed curve relates to the ocean scene and the solid curve to the Sahara scene.

Obviously, the errors are small ($\leq 1\%$) in the wavelength region of interest (500–800 nm). Note the strong peak at 305 nm. It is related to the transition from strong ozone absorption below 300 nm to pure Rayleigh scattering above ~ 330 nm.¹⁴ Although the errors presented in Fig. 6 were calculated for specific scenes, they are representative of most other situations. In conclusion, the difference in solar geometry due to the time delay in between the overpasses of GOME and SCIAMACHY does not have a significant effect on the reflectance comparison of this paper.

6. Conclusion

In this paper we performed an intercomparison of the reflectances of two satellite spectrometers, namely,

GOME and SCIAMACHY. The accuracy of the comparison method is increased by focusing on carefully selected Earth targets, in this case a cloud-free scene over a homogeneous part of the Sahara Desert. The effect of the different solar angles for observations by GOME and SCIAMACHY is investigated and found to be well below 1%. We estimate the accuracy of the results to be well within 5%.

The final results indicate that there is disagreement between GOME and SCIAMACHY over their entire mutual wavelength range. However, we have to restrict our conclusions about the quality of the radiometric calibration of SCIAMACHY to the wavelength region of 500–800 nm because GOME is suffering from a severe degradation in the UV, up to 500 nm. For the wavelength region of 500–800 nm, where GOME is reliable, we find a difference of 15%–20% in the reflectances. We attribute this completely to SCIAMACHY, which is known to be suffering from calibration errors.^{14,15,18,21,22} Further evidence is found from a comparison between the imager MERIS and SCIAMACHY,¹⁸ the results of which closely agree with ours.

We would like to end this conclusion with an illustration of the importance of a proper absolute calibration of the Earth's reflectance. The Fast Retrieval Scheme for Clouds from the Oxygen A-band (FRESCO) algorithm¹¹ provides cloud information and makes use of the oxygen A band (between 758 and 775 nm). For SCIAMACHY, the algorithm only converges and produces a good level 2 cloud product when the SCIAMACHY reflectance around 765 nm is multiplied by a factor of 1.2.³⁰ Note that this is exactly the same correction factor we find from Fig. 3 at 765 nm.

This work was financed by the Netherlands Agency for Aerospace Programmes and the Space Research Organisation Netherlands through project EO-076. We thank the European Space Agency and the Deutsches Zentrum für Luft- und Raumfahrt for providing the GOME and SCIAMACHY data.

References

1. J. P. Burrows, M. Weber, M. Buchwitz, V. Rozanov, A. Ladstätter-Weißemayer, A. Richter, R. de Beek, R. Hoogen, K. Bramstedt, K.-U. Eichman, M. Eisinger, and D. Perner, "The Global Ozone Monitoring Experiment (GOME): mission concept and first scientific results," *J. Atmos. Sci.* **56**, 151–175 (1999).
2. H. Bovensmann, J. P. Burrows, M. Buchwitz, J. Frerick, S. Noël, V. V. Rozanov, K. V. Chance, and A. P. H. Goede, "SCIAMACHY: mission objectives and measurement modes," *J. Atmos. Sci.* **56**, 127–150 (1999).
3. P. Stammes, P. F. Levelt, J. de Vries, H. Visser, B. Kruizinga, C. Smorenburg, G. W. Leppelmeier, and E. Hilsenrath, "Scientific requirements and optical design of the Ozone Monitoring Instrument on EOS-CHEM," in *Earth Observing Systems IV*, W. L. Barnes, ed., Proc. SPIE **3750**, 221–232 (1999).
4. U. Platt, "Differential Optical Absorption Spectroscopy (DOAS)," in *Air Monitoring by Spectroscopic Techniques*, Vol. 127 of Chemical Analysis Series, M. W. Sigrist, ed. (Wiley, 1994), pp. 27–84.
5. R. Munro, R. Siddans, W. J. Reburn, and B. J. Kerridge, "Di-

- rect measurements of tropospheric ozone distributions from space," *Nature* **392**, 168–171 (1998).
6. R. Hoogen, V. V. Rozanov, and J. P. Burrows, "Ozone profiles from GOME satellite data: algorithm description and first validation," *J. Geophys. Res.* **104D**, 8263–8280, doi:10.1029/1998JD100093 (1999).
 7. R. J. D. Spurr, "Linearized radiative transfer theory: a general discrete ordinate approach to the calculation of radiances and analytic weighting functions, with application to atmospheric remote sensing," Ph.D. dissertation (Technical University Eindhoven, The Netherlands, 2001).
 8. R. J. van der A, R. F. van Oss, A. J. M. Pijters, J. P. F. Fortuin, Y. J. Meijer, and H. M. Kelder, "Ozone profile retrieval from recalibrated Global Ozone Monitoring Experiment data," *J. Geophys. Res.* **107D**, 4239, doi:10.1029/2001JD000696 (2002).
 9. O. P. Hasekamp, J. Landgraf, and R. van Oss, "The need of polarization modeling for ozone profile retrieval from backscattered sunlight," *J. Geophys. Res.* **107D**, 4692, doi:10.1029/2002JD002387 (2002).
 10. Y. J. Meijer, R. J. van der A, R. F. van Oss, D. P. J. Swart, H. M. Kelder, and P. V. Johnston, "Global Ozone Monitoring Experiment ozone profile characterization using interpretation tools and lidar measurements for intercomparison," *J. Geophys. Res.* **108D**, 4723, doi:10.1029/2003JD003498 (2003).
 11. R. B. A. Koelemeijer, P. Stammes, J. W. Hovenier, and J. F. de Haan, "A fast method for retrieval of cloud parameters using oxygen A band measurements from the Global Ozone Monitoring Experiment," *J. Geophys. Res.* **106D**, 3475–3490, doi:10.1029/2000JD900657 (2001).
 12. J. R. Acarreta, P. Stammes, and W. H. Knap, "First retrieval of cloud phase from SCIAMACHY spectra around 1.6 micron," *Atmos. Res.* **72**, 89–105 (2004).
 13. M. de Graaf, P. Stammes, O. Torres, and R. B. A. Koelemeijer, "Absorbing aerosol index: sensitivity analysis, application to GOME and comparison with TOMS," *J. Geophys. Res.* **110**, D01201, doi:10.1029/2004JD005178 (2005).
 14. L. G. Tilstra, G. van Soest, and P. Stammes, "Method for in-flight satellite calibration in the ultraviolet using radiative transfer calculations, with application to Scanning Imaging Absorption Spectrometer for Atmospheric Chartography (SCIAMACHY)," *J. Geophys. Res.* **110**, D18311, doi:10.1029/2005JD005853 (2005).
 15. G. van Soest, L. G. Tilstra, and P. Stammes, "Large-scale validation of SCIAMACHY reflectance in the ultraviolet," *Atmos. Chem. Phys.* **5**, 2171–2180 (2005).
 16. B. Kerridge, R. Siddans, J. Reburn, B. Latter, and V. Jay, "Intercomparisons of MIPAS and SCIAMACHY L1 and L2 products with GOME and AATSR," presented at the Envisat Validation Workshop, Frascati, Italy, 9–13 December 2002.
 17. R. Snel, "In-orbit optical path degradation: GOME experience and SCIAMACHY prediction," in *Proceedings of the ERS-Envisat Symposium*, ESA Spec. Publ. SP-461 (European Space Agency, 2000).
 18. J. R. Acarreta and P. Stammes, "Calibration comparison between SCIAMACHY and MERIS onboard ENVISAT," *IEEE Geosci. Remote Sens. Lett.* **2**, 31–35, doi:10.1109/LGRS.2004.838348 (2005).
 19. I. Aben, M. Eisinger, E. Hegels, R. Snel, and C. Tanzi, "GOME Data Quality Improvement GDAQI final report," Rep. TN-GDAQI-003SR/2000 (European Space Agency, 2000).
 20. R. Santer, N. Martiny, and I. Smolskaia, "Vicarious calibration of MERIS over dark waters in the near infrared," in *Proceedings of the 2004 Envisat and ERS Symposium*, ESA Spec. Publ. SP-572 (European Space Agency, 2004).
 21. S. Noël, "Determination of correction factors for SCIAMACHY radiances and irradiances," Tech. Note IFE-SCIA-SN-20040514 (University of Bremen, Bremen, Germany, 2004).
 22. W. Gurliit, H. Bösch, H. Bovensmann, J. P. Burrows, A. Butz, C. Camy-Peyret, M. Dorf, K. Gerilowski, A. Lindner, S. Noël, U. Platt, F. Weidner, and K. Pfeilsticker, "The UV-A and visible solar irradiance spectrum: inter-comparison of absolutely calibrated, spectrally medium resolution solar irradiance spectra from balloon- and satellite-borne measurements," *Atmos. Chem. Phys.* **5**, 1879–1890 (2005).
 23. J. F. de Haan, P. B. Bosma, and J. W. Hovenier, "The adding method for multiple scattering calculations of polarised light," *Astron. Astrophys.* **183**, 371–391 (1987).
 24. P. Stammes, "Spectral radiance modelling in the UV-visible range," in *IRS 2000: Current Problems in Atmospheric Radiation*, W. L. Smith and Y. M. Timofeyev, eds. (Deepak, 2001), pp. 385–388.
 25. R. B. A. Koelemeijer, J. F. de Haan, and P. Stammes, "A database of spectral surface reflectivity in the range 335–772 nm derived from 5.5 years of GOME observations," *J. Geophys. Res.* **108D**, 4070, doi:10.1029/2002JD002429 (2003).
 26. R. J. van der A, H. J. Eskes, J. H. G. M. van Geffen, R. F. van Oss, A. J. M. Pijters, P. J. M. Valks, and C. Zehner, "GOME Fast Delivery and Value-Added Products (GOFAP)," in *Proceedings of the ERS-Envisat Symposium*, ESA Spec. Publ. SP-461 (European Space Agency, 2000).
 27. H. J. Eskes, R. J. van der A, E. J. Brinksma, J. P. Veefkind, J. F. de Haan, and P. J. M. Valks, "Retrieval and validation of ozone columns derived from measurements of SCIAMACHY on Envisat," *Atmos. Chem. Phys. Discuss.* **5**, 4429–4475 (2005).
 28. Troposphere Emission Monitoring Internet Service (TEMIS), <http://www.temis.nl/>.
 29. G. P. Anderson, S. A. Clough, F. X. Kneizys, J. H. Chetwynd, and E. P. Shettle, "AFGL atmospheric constituent profiles (0–120 km)," Environment Research Paper 954, Rep. AFGL-TR-86-0110 (U.S. Air Force Geophysics Laboratory, Hanscom Air Force Base, Mass., 1986).
 30. N. Fournier, P. Stammes, M. de Graaf, R. J. van der A, A. J. M. Pijters, R. B. A. Koelemeijer, and A. A. Kokhanovsky, "Improving cloud information over deserts from SCIAMACHY O₂ A-band," *Atmos. Chem. Phys. Discuss.* **5**, 6013–6039 (2005).